
A Simple Plug-in for Improving Eviction-Based KV Cache Compression

Yuping Lin^{1*} Jiayuan Ding² Yue Xing¹ Pengfei He¹
Jiliang Tang¹ Subhabrata Mukherjee²

¹Michigan State University ²Hippocratic AI

{linyupin,xingyue1,hepengf1,tangjili}@msu.edu
{jiayuan,subho}@hippocraticai.com

Abstract

KV cache growth is a major bottleneck for long-context inference in large language models. Existing methods are often dominated by binary eviction or representation approximation, which may underutilize tokens that are not critical for exact retention but are still reconstructable. We present VECTOR, a plug-and-play augmentation for eviction-based pipelines that introduces three-way token routing: retention, approximation, and eviction. VECTOR combines an importance signal from the base scorer with a reconstructability signal from an offline-calibrated regression-based value estimation. By leveraging reconstructability, VECTOR recovers useful value information that would otherwise be irreversibly lost under binary eviction, while preserving key vectors for attention routing stability. Experimental results show that VECTOR improves quality-memory trade-offs under medium-to-high compression, with especially clear gains in stricter budget regimes.

1 Introduction

Large language models (LLMs) increasingly rely on long-context inference [1, 2, 3], yet their key-value (KV) cache grows linearly with sequence length and quickly becomes the dominant memory cost [4, 5]. This bottleneck limits practical deployment in many applications such as retrieval-heavy QA [6], agent workflows [7], and multi-turn reasoning [8], where context windows are long and memory budgets are strict. As a result, KV cache compression has become a central system problem for long-context LLM serving [4].

Existing KV compression methods mainly follow two strategies. The first strategy is *importance-based eviction*, where tokens are scored and low-score entries are permanently evicted (e.g., SnapKV [9], KeyDiff [10], KVzip [11]). While these methods are simple and efficient, their decision is inherently binary: tokens are either fully retained or completely discarded. Under tight budgets, such an irreversible eviction can substantially degrade downstream performance, especially when recent multi-state systems such as ARKV [12] and D2O [13] suggest that non-binary allocation can outperform pure eviction.

The second strategy is *representation approximation*, which compresses KV representations through quantization, projection, or reconstruction (e.g., AQUA-KV [14], EliteKV [15], DeltaKV [16], Attention Matching [17]). Rather than removing tokens outright, these methods attempt to preserve information approximately after compression. However, many existing approaches require architectural modifications, retraining, or expensive online computation, such as retrieval-based reconstruction [16], context-dependent fitting [17], or model uptraining [15].

*Work done during internship at Hippocratic AI.

To better balance memory reduction and downstream performance, we treat KV compression as a unified *retain–approximate–evict* allocation problem, where tokens are selectively retained, approximately reconstructed, or removed under a fixed memory budget. This perspective is motivated by two observations. First, recent multi-state methods [12, 13] demonstrate that non-binary allocation outperforms pure eviction. However, their allocation decisions are driven by token importance signals such as attention scores or attention statistics. They do not explicitly model *reconstructability*, namely, whether a token’s KV representation can be accurately recovered from other available information with limited error. This distinction matters because not all important tokens are equally compressible: some can be safely approximated, while others are highly error-sensitive and should instead be retained exactly. Second, prior work on KV quantization suggests that keys and values exhibit asymmetric sensitivity to compression error, with values generally being more tolerant to approximation than keys [18, 19]. However, existing token-level KV compression methods rarely exploit this asymmetry explicitly when allocating memory across tokens. This enables the potential to improve both performance and compression efficiency.

Motivated by these challenges, we raise two research questions. The first concerns the approximation mechanism; the second concerns the allocation strategy.

- **RQ1:** Can we build a lightweight reconstruction mechanism that recovers value representations with low runtime overhead and no architectural retraining?
- **RQ2:** Under a fixed KV memory budget, how should we jointly use *importance* and *reconstructability* to allocate tokens into *retention*, *approximation*, and *eviction* tiers?

To answer these questions, we propose **VECTOR** (Value Estimation via Collinearity and Three-way Orthogonal Routing), a plug-and-play augmentation for token-importance-based eviction methods. Unlike multi-state methods such as ARKV [12] and D2O [13], which are standalone compression pipelines driven by importance signals alone, VECTOR augments existing eviction backbones by introducing reconstructability as a second allocation dimension.

For **RQ1**, VECTOR uses an offline-calibrated Ordinary Least Squares (OLS) to reconstruct values from keys. Since keys and values are both linear projections of the same hidden state, they share an intrinsic low-rank structure that makes linear prediction feasible. This choice is based on the asymmetric sensitivity of attention: keys determine the softmax allocation weights, where perturbations can be amplified nonlinearly. Values, in contrast, are aggregated linearly under those weights [18, 19]. Accordingly, VECTOR preserves keys for allocation stability and reconstructs values on demand through a fixed linear transformation.

For **RQ2**, VECTOR performs budgeted three-way allocation on two orthogonal axes: token *importance* (from a base eviction policy) and token *reconstructability* (from OLS reconstruction error). Intuitively, hard-to-reconstruct tokens should be retained, easy-to-reconstruct tokens can be approximated, and low-importance tokens can be evicted. Under the same KV memory budget, this reconstructability-aware allocation recovers part of the information that binary eviction would discard, enabling better quality-memory trade-offs under high compression.

Our main contributions are summarized as follows:

- **A reconstructability-aware allocation view of KV compression.** As in Figure 1, we formulate KV budget allocation as a three-way token allocation problem that jointly considers *importance* and *reconstructability*, rather than a binary *retention/eviction* decision.
- **A lightweight $K \rightarrow V$ reconstruction module.** We develop a one-time offline OLS calibration that enables online value reconstruction from the stored keys, with low inference-time overhead.
- **A plug-and-play upgrade for eviction baselines.** VECTOR can be attached to representative token-importance eviction methods (e.g., attention-score-based and key-geometry-based) with minimal integration adaptations.

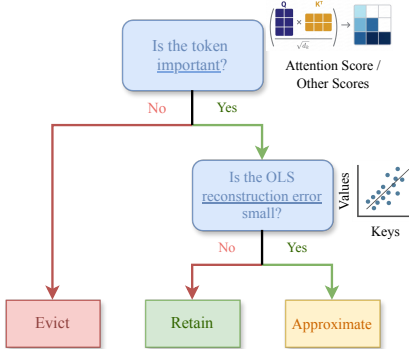


Figure 1: Overview of VECTOR’s three-way token allocation. The base importance scorer first filters out unimportant tokens for eviction. For important tokens, VECTOR evaluates OLS-based $K \rightarrow V$ reconstruction error: tokens with small error enter *Approximation*, while tokens with large error remain in *Retention*. Approximation is applied to values only (V-only), with keys retained.

- **Empirical gains under strict memory budgets.** Experiments on long-context benchmarks show that adding VECTOR to existing eviction baselines improves downstream performance in high-compression regimes across our evaluated settings.

2 Related Works

KV Cache Compression Existing methods fall into three families. Eviction-based methods score tokens by importance and permanently discard low-scoring entries [5, 9, 10, 20, 11]. They are effective but operate as binary keep-or-drop policies, causing irreversible information loss under tight budgets. Quantization methods reduce bit-width across all cached entries [18, 21, 19, 14]. They are less destructive but bounded in compression ratio and often require hardware support. Approximation methods reconstruct KV representations through low-rank projection or residual modeling [22, 16, 17, 15]. Recent multi-state designs such as ARKV and D2O show that non-binary allocation increasingly matters under aggressive compression [12, 13].

Exploiting K–V Subspace Redundancy Since K and V are both projected from the same hidden state, their shared structure can be exploited for compression. MLA compresses token memory into a shared latent representation [23]. AQUA-KV and EliteKV leverage K/V dependency through residual quantization and joint low-rank projection, respectively [14, 15]. These works support the view that K–V asymmetry is a practically exploitable property.

Relation to Our Method VECTOR is a plug-and-play augmentation for eviction-based pipelines, not a standalone compression method. Unlike approximation-oriented approaches [22, 16], it requires no architectural modification or retraining and preserves full compatibility with existing eviction backbones. Within the eviction family, VECTOR extends binary retain/eject decisions by introducing a third approximation tier driven by reconstructability, a dimension that prior multi-state methods [12, 13] do not explicitly model. We therefore evaluate VECTOR as an augmentation over eviction baselines, which directly reflects its intended use case.

3 Method

VECTOR extends token-importance-based eviction method by introducing a third allocation state: *approximation*. As in Figure 1, token routing proceeds along two dimensions. The first is *importance*, provided by a base eviction scorer. The second is *reconstructability*, which measures how accurately a token’s value can be recovered from its key via a lightweight linear predictor. Together, these two dimensions determine whether each token is retained exactly, approximated, or evicted.

The remainder of this section is organized as follows. Section 3.1 describes the value estimation mechanism that makes approximation possible. Section 3.2 presents the full VECTOR pipeline that integrates both dimensions into a budgeted three-way allocation.

3.1 Approximation: Value Estimation via K–V Collinearity

While the above discussion motivates the incorporation of *reconstructability* into KV cache compression, it is crucial to recognize that keys and values exhibit different tolerances to approximation errors. Recent studies [19, 24] have shown that even small perturbations in key vectors are exponentially amplified by the softmax function, leading to catastrophic disruptions in the attention probability distribution. In contrast, errors in value vectors propagate only linearly through the weighted sum, as values are applied after the softmax normalization. This asymmetry suggests that approximating keys is significantly more risky than approximating values.

Building on this observation, we adopt a *V-only estimation* strategy for tokens in the *Approximation* state. Specifically, we retain the exact key vector to preserve the integrity of the attention routing mechanism, while discarding the original value vector to reclaim memory. The missing value is subsequently reconstructed using an alternative compact representation. This asymmetric treatment ensures that the critical attention map remains uncompromised while maximizing memory savings. We empirically validate this design choice in Appendix E, where K-only approximation shows inconsistent gains and occasionally degrades below the unaugmented baseline under medium-to-high compression, while V-only approximation consistently improves over it.

To validate this approach, we provide an empirical evidence in the following.

Empirical Evidence Before presenting the full method design, we first verify a prerequisite of our approach: *whether a simple linear map can reliably predict V from K across different model families, scales, and architectures.* We employ the C4 dataset [25], a large-scale pre-training corpus, to collect key and value activation vectors at each transformer layer, drawing from 10,000 sequences of 4,096 tokens. For each layer, a linear model predicting V from K is subsequently fitted via OLS regression. To evaluate generalization, we additionally construct a held-out test set consisting of 100 sequences of 4,096 tokens, and report the mean R^2 of the OLS averaged across all layers within each model on this test set. As shown in Table 1, offline OLS achieves high $K \rightarrow V$ predictability on all tested models, with R^2_{global} ranging from 0.6863 to 0.9392. This result serves as the empirical foundation of our approximation strategy.

Table 1: Cross-model $K \rightarrow V$ predictability with offline OLS. We report layer-averaged R^2_{global} for each model, showing high linear predictability across model families, scales, and architectures.

Model	R^2_{global} (All-Layer Avg.)
Llama-3.1-8B	0.6964
Qwen3-14B	0.6946
Qwen3-0.6B	0.9392
Gemma-3-4B	0.8896
Qwen3-30B-A3B	0.6863

Remark In standard attention mechanisms, both $K \in \mathbb{R}^{d_k}$ and $V \in \mathbb{R}^{d_v}$ are linear projections of the same input hidden state $h \in \mathbb{R}^d$, i.e., $K = W_K h$ and $V = W_V h$.² In principle, V could be exactly reconstructed from K if the projection matrices were invertible and $d_v = d_k = d$. However, this condition is rarely satisfied in practice, as modern architectures typically use $d_k, d_v \ll d$ for computational efficiency [26, 27, 28, 1].

Despite this dimensional reduction, recent studies on representation learning have revealed the “massive activations” phenomenon [29], showing that although the nominal dimension d of h is large, its variance is dominated by a low effective rank. Besides, the existing Multi-Head Latent Attention (MLA) architecture [23] explicitly enforces a shared low-dimensional latent representation for both K and V . All the above imply that the intrinsic dimensionality of h is much smaller than d , and consequently, both K and V can be well-approximated by projections of a shared low-dimensional subspace. Therefore, even when d_k and d_v are much smaller than d , it remains feasible to predict V from K by exploiting this underlying low-rank structure.

Analytical Pseudo-Inverse vs. Data-Driven OLS Given $K = W_K h$ and $V = W_V h$, a natural approach is to first reconstruct h from K and subsequently obtain V via W_V . The Moore-Penrose (MP) pseudo-inverse $W_{\text{MP}} = W_K^\top (W_K W_K^\top)^{-1}$ offers a closed-form solution $\hat{V} = W_V W_{\text{MP}} K$. However, this approach does not directly optimize the target prediction error of \hat{V} . Specifically, the MP pseudo-inverse yields the minimum ℓ_2 -norm solution to the system $W_K h' = K$, i.e., it solves $\min_{h'} \|W_K h' - W_K h\|_2^2$ and, among all exact solutions, selects the one with minimal $\|h'\|_2$. This objective is fundamentally different from minimizing the V -prediction error $\|W_V h - W_V h'\|_F^2$: the latter involves a distinct linear transformation (W_V rather than W_K), which in general induces a different geometry on the residual. Therefore, W_{MP} provides no guarantee of minimizing the error in predicting V .

To this end, we instead directly learn an Ordinary Least Squares (OLS) estimator W_{OLS} by minimizing the prediction error in V -space:

$$W_{\text{OLS}} = \arg \min_W \mathbb{E}_{h \sim \mathcal{D}} \|W K - V\|_F^2.$$

where \mathcal{D} denotes the distribution of hidden states h induced by a large-scale, diverse pre-training corpus. This data-driven approach directly minimizes the V -prediction error, unlike the pseudo-inverse which optimizes a different objective. As shown in Appendix D, OLS substantially outperforms the analytical pseudo-inverse in $K \rightarrow V$ predictability across all tested models.

RoPE Decoupling A critical engineering challenge arises with Rotary Position Embedding (RoPE) [30], which is ubiquitously adopted in modern LLMs. RoPE applies a position-dependent rotation to the keys ($K_{\text{post-RoPE}} = R_m W_K h$ at position m), while values remain position-independent

²Throughout this paper, we denote all vectors as column vectors, and linear transformations are written as $y = Wx$.

($V = W_V h$). Fitting a static OLS matrix directly on post-RoPE keys would necessitate position-dependent estimators due to the entanglement of positional information, adding unnecessary complexity. To expose the intrinsic K-V collinearity, we explicitly decouple the positional information by applying an inexpensive inverse rotation ($R_m^{-1} K_{\text{post-RoPE}}$) to the cached keys during the approximation phase. This lightweight decoupling allows the static W_{OLS} to accurately reconstruct V regardless of token position.

3.2 The VECTOR Pipeline

In the following, we introduce the complete VECTOR pipeline for the three-way allocation. The pipeline is designed as a lightweight, plug-and-play extension that augments existing token-importance-based eviction algorithm (e.g., SnapKV [9], KVzip [11], KeyDiff [10]).

Denote p_c as the target memory compression ratio. To incorporate the *Approximation* state while preserving the same memory budget, VECTOR executes the following three-step pipeline:

Step 1: Budget Relaxation. Let p_a denote the approximation ratio. VECTOR invokes the base token-importance eviction algorithm to identify an expanded candidate pool of size $1 - p_c + p_a$. This yields a larger initial set of contextually relevant tokens, from which we subsequently determine which ones to compress.

Step 2: Residual Evaluation. For each token in the expanded candidate pool, VECTOR computes the per-token reconstruction error $\varepsilon_i = \|V_i - W_{\text{OLS}} K_i\|_2^2$ using the offline-calibrated OLS projection matrix W_{OLS} . This step introduces an orthogonal dimension of evaluation—*reconstructability*—that quantifies the approximation error incurred if the token’s value were discarded.

Step 3: Asymmetric Truncation. As illustrated in Figure 2, VECTOR partitions the expanded pool based on the computed reconstruction errors to execute the budget swap:

- The keys of *all* $1 - p_c + p_a$ tokens in the expanded pool are retained.
- The $2p_a$ tokens with the lowest reconstruction errors ε_i (i.e., those most amenable to approximation) have their cached values discarded. During generation, these values are dynamically reconstructed via $\hat{V} = W_{\text{OLS}} K$.
- Both keys and values are exactly retained for the remaining $1 - p_c - p_a$ proportion of tokens.

Through the above procedure, $1 - p_c + p_a$ keys and $1 - p_c - p_a$ values are stored in memory, consuming the exact same footprint as $1 - p_c$ full KV pairs. Specifically, the *Eviction*, *Approximation*, and *Retention* states account for proportions $p_c - p_a$, $2p_a$, and $1 - p_c - p_a$ of all tokens, respectively. The choice of p_a is discussed in Section 4, along with a sensitivity analysis in Section 5.3.

4 Theoretical Analysis

We analyze the effect of introducing the *Approximation* state under a fixed memory budget. The central question is: under what conditions does expanding the *Approximation* tier reduce information loss, compared to binary eviction?

To formalize this, we define \mathcal{E} as an importance-weighted measure of signal loss after compression. An evicted token contributes a full loss of 1 to \mathcal{E} . A retained token contributes 0. An approximated token contributes its normalized reconstruction error $\|V_i - \hat{V}_i\|_2^2 / \|V_i\|_2^2 \in [0, 1]$. A smaller \mathcal{E} means less distortion to the attention computation.

We then characterize when expanding the *Approximation* state reduces \mathcal{E} (Proposition 1). The key quantity is R_{approx}^2 , the OLS prediction quality measured specifically over the tokens selected for approximation. Intuitively, R_{approx}^2 close to 1 means approximated tokens are well-reconstructed, contributing little to \mathcal{E} . We derive a threshold on R_{approx}^2 that depends on the skewness of the

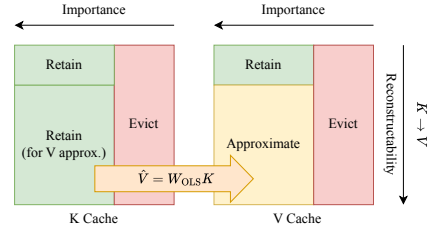


Figure 2: Asymmetric three-way allocation: K is retained exactly for the expanded candidate pool, while V is split into *Retain*, *Approximate*, and *Evict*.

importance score distribution. We also provide a closed-form expression for \mathcal{E} under a Gaussian residual assumption (Example 1).

Let $\mathcal{I}_E(p_a, p_c)$ and $\mathcal{I}_A(p_a, p_c)$ denote the index sets of evicted and approximated tokens, respectively, and let w_i denote the importance score of the i -th token. We then write \mathcal{E} as:

$$\begin{aligned} \mathcal{E}(p_a, p_c) &= \sum_{i \in \mathcal{I}_E(p_a, p_c)} w_i + \sum_{i \in \mathcal{I}_A(p_a, p_c)} w_i \frac{\|V_i - \hat{V}_i\|_2^2}{\|V_i\|_2^2} \\ &\approx \sum_{i \in \mathcal{I}_E(p_a, p_c)} w_i + \left(\sum_{i \in \mathcal{I}_A(p_a, p_c)} w_i \right) \cdot \mu_A, \end{aligned}$$

where the approximation assumes that the per-token reconstruction errors $\|V_i - \hat{V}_i\|_2^2 / \|V_i\|_2^2$ are approximately independent of the importance scores w_i , and $\mu_A = 1 - R_{\text{approx}}^2(p_a, p_c)$ denotes the mean relative reconstruction error over \mathcal{I}_A . Here, $R_{\text{approx}}^2(p_a, p_c)$ is the R^2 computed solely over the tokens in the *Approximation* set.

The following proposition characterizes the relationship among R_{approx}^2 , the importance score distribution, and the overall distortion \mathcal{E} . Specifically, we derive the condition on R_{approx}^2 under which expanding the *Approximation* state reduces \mathcal{E} , and show that this condition depends on the skewness of the importance score distribution.

Proposition 1. *Let $\bar{w} = (1 - \sum_{i \in \mathcal{I}_E} w_i) / (1 - p_c + p_a)$ be the average importance score of the tokens in the expanded pool, and let w^* be the importance score of the token at the truncation boundary of the Eviction set. Expanding the Approximation state reduces the global distortion if:*

$$R_{\text{approx}}^2 > \frac{\bar{w}}{w^* + \bar{w}}.$$

Based on Proposition 1, the required predictability R_{approx}^2 is governed by the skewness of the importance score distribution. When expanding the *Approximation* tier, tokens enter from both the *Eviction* set (gaining recovery) and the *Retention* set (incurring approximation error). For highly skewed distributions where $\bar{w} \gg w^*$, the latter effect dominates, and OLS must achieve higher accuracy to compensate and yield a net reduction in distortion.

Besides the above, the following example adopts a Gaussian assumption on the OLS residuals to examine how the shape of the residual distribution affects R_{approx}^2 and, consequently, \mathcal{E} :

Example 1. *Let ϕ and Φ denote the PDF and CDF of the standard normal distribution, respectively. Let r_i denote the signed OLS residual for the i -th token, satisfying $r_i^2 = \|V_i - \hat{V}_i\|_2^2 = \varepsilon_i$. Assume $r_i \stackrel{\text{i.i.d.}}{\sim} \mathcal{N}(0, \sigma^2)$, and let Σ^2 denote the variance of $\|V_i\|_2$ ($\Sigma^2 > \sigma^2$). Define $\eta(p_a, p_c) := \sigma \Phi^{-1}(1/2 + p_a/(1 - p_c + p_a))$. Then, given a target retention ratio $1 - p_c$:*

$$\mathcal{E}(p_a, p_c) \approx \sum_{i \in \mathcal{I}_E(p_a, p_c)} w_i + \underbrace{2p_a \bar{w} \frac{\sigma^2}{\Sigma^2} \left(1 - \frac{2(\eta(p_a, p_c)/\sigma) \phi(\eta(p_a, p_c)/\sigma)}{2p_a/(1 - p_c + p_a)} \right)}_{1 - R_{\text{approx}}^2(p_a, p_c)},$$

showing that $1 - R_{\text{approx}}^2(p_a, p_c)$ depends on σ^2 and Σ^2 under the Gaussian distribution.

Combining Proposition 1 and Example 1, when the importance score distribution concentrates on the *Approximation* and *Retention* sets (i.e., $\bar{w} \gg w^*$), the method is effective provided that the values are highly predictable from the keys, i.e., $\sigma^2 \ll \Sigma^2$.

For deployment, since the KV cache varies across samples, w^* and \bar{w} change accordingly, making it impractical to determine p_a dynamically. We therefore adopt the following empirical formula:

$$p_a^{\text{deploy}} = \min(p_c/2, (1 - p_c - \epsilon)/2), \quad (1)$$

where $\epsilon > 0$ is a small constant ensuring a non-empty *Retention* tier. The first term keeps the *Approximation* tier no larger than half the compressed budget, and the second ensures sufficient headroom for the *Retention* tier.

Table 2: LongBench results for four eviction baselines and their VECTOR-augmented variants under compression ratios $p_c \in \{0.25, 0.50, 0.75, 0.90\}$. Approximation ratios are set by Eq. 1. Results for Qwen3-0.6B are provided in Appendix A.

		LongBench																	
Method	Comp. Ratio	narrativeqa	qasper	multifield-qa_en	hotpotqa	2wikimqa	musicqa	gov_report	qmsum	multi_news	trec	triviaqa	samsun	passage_count	passage_retrieval_en	lcc	rebench-p	Avg.	
Llama-3.1-8B	No Comp.	30.59	46.93	55.94	59.04	51.99	33.17	35.22	25.19	26.84	29.00	91.56	40.11	10.15	100.00	51.28	44.11	45.69	
	0.25	31.27	47.30	53.98	58.39	50.69	34.08	34.54	24.51	26.80	63.00	92.71	41.46	11.15	100.00	49.04	44.23	47.70	
	0.50	32.46	45.65	52.60	56.07	46.20	28.62	32.98	24.33	25.79	64.00	92.71	41.28	10.15	99.50	42.65	43.48	46.15	
	0.75	29.14	31.75	43.25	52.83	38.74	24.69	29.36	23.37	22.99	49.50	91.93	40.01	10.56	99.50	34.33	44.44	41.65	
	0.90	27.53	17.00	34.69	40.03	26.18	16.01	26.12	21.28	18.89	40.00	92.24	40.30	9.50	89.00	21.33	44.34	35.28	
	0.25	30.60	48.18	56.07	58.45	50.72	33.59	34.80	24.74	26.90	34.50	92.71	41.17	10.65	99.50	51.63	44.29	46.16	
	0.50	32.24	47.38	56.77	58.92	51.65	35.47	32.99	24.68	26.10	59.00	92.49	40.54	10.63	99.50	50.73	43.78	47.68	
	0.75	30.54	39.20	53.15	54.83	45.85	28.83	29.55	23.79	24.03	56.50	91.87	39.67	10.58	98.50	46.56	44.26	44.86	
	0.90	28.12	23.96	37.98	49.88	30.72	20.72	25.75	22.39	20.43	43.00	91.19	39.10	12.05	94.50	35.20	45.03	38.75	
	0.25	30.59	46.85	56.24	58.64	52.63	32.54	34.28	25.08	26.44	32.00	91.56	40.85	10.20	100.00	51.62	44.36	45.87	
	0.50	30.39	46.56	55.62	58.99	52.54	33.01	32.77	24.85	25.52	35.50	91.88	40.24	12.15	100.00	50.73	43.54	45.89	
	0.75	29.79	44.40	54.79	58.79	50.49	32.63	29.65	24.28	23.37	40.00	91.78	40.54	10.63	100.00	52.01	45.05	45.51	
	0.90	31.04	38.72	52.98	56.19	45.95	27.55	26.02	23.57	19.73	36.00	91.09	39.70	9.55	99.50	48.65	47.78	43.38	
	0.25	31.31	47.23	55.62	59.42	51.19	31.27	34.64	25.01	26.69	27.00	91.88	40.13	10.65	100.00	50.97	44.30	45.46	
	0.50	31.93	47.52	56.78	59.48	51.04	31.02	33.11	25.09	26.19	25.00	91.95	38.49	10.60	99.50	48.56	44.94	45.08	
	0.75	31.96	46.80	56.70	58.29	50.12	30.47	31.44	24.13	23.00	91.71	39.67	9.63	99.50	48.44	45.32	45.11		
	0.90	30.36	43.94	54.65	55.96	48.54	31.06	28.17	24.91	22.17	42.50	90.15	40.00	11.50	99.50	50.89	49.06	45.20	
	0.25	30.88	48.12	56.35	59.01	49.82	32.53	34.58	25.27	26.81	19.50	91.37	38.04	11.38	100.00	54.46	45.59	45.23	
	0.50	30.87	47.64	57.01	55.67	49.32	28.62	35.14	25.14	27.27	15.50	88.53	34.42	10.19	100.00	50.76	44.97	43.82	
	0.75	32.38	45.70	54.79	56.35	47.38	25.80	34.35	25.16	26.64	46.00	86.48	32.59	11.80	99.00	49.41	45.42	44.95	
	0.90	29.93	40.28	53.83	52.65	39.23	26.38	31.77	23.68	25.66	45.00	90.63	37.69	10.50	59.50	42.06	50.83	41.23	
	0.25	32.45	49.88	56.76	58.51	50.08	33.50	34.58	25.14	27.18	18.50	91.37	38.80	12.29	99.00	53.98	44.79	45.49	
	0.50	32.32	48.04	57.55	56.20	52.02	34.30	33.73	24.85	26.71	13.50	92.64	39.55	10.04	99.00	53.48	45.36	45.08	
	0.75	32.16	47.06	55.82	56.23	50.47	29.46	33.55	24.86	26.78	39.00	87.76	35.06	10.25	100.00	49.11	44.70	45.11	
	0.90	30.18	44.07	55.41	53.23	46.03	28.48	31.65	24.11	25.70	58.00	90.41	39.33	10.25	88.00	49.18	49.24	45.20	
	0.25	31.37	48.20	56.60	55.38	53.59	28.34	34.61	25.00	26.54	53.00	93.44	40.79	12.50	100.00	52.28	49.40	47.56	
	0.50	30.63	46.84	56.98	56.00	52.77	26.87	32.01	25.26	25.05	50.00	93.44	40.65	12.50	100.00	53.11	49.48	46.97	
	0.75	30.80	44.30	55.63	55.77	52.30	28.99	29.21	24.64	23.37	44.00	93.14	40.18	12.00	100.00	52.84	48.79	46.00	
	0.90	30.38	38.20	52.49	55.83	45.69	27.28	25.54	23.73	19.77	36.00	92.77	39.98	11.55	99.50	48.78	48.85	43.52	
	0.25	30.67	48.51	57.72	55.66	54.38	28.68	34.74	25.36	26.45	51.50	93.37	40.34	12.50	99.50	53.29	49.36	47.63	
	0.50	31.87	49.23	57.69	55.47	52.18	27.39	31.71	25.03	24.83	54.50	93.37	39.07	12.00	99.50	49.61	47.31	47.31	
	0.75	30.23	45.69	56.14	57.11	50.11	26.61	29.50	24.81	22.59	56.00	93.37	40.22	11.00	99.50	52.78	48.89	46.54	
	0.90	28.85	43.13	54.43	56.22	47.83	27.24	26.96	24.29	20.47	48.50	93.45	40.69	10.00	99.50	50.85	48.51	45.06	
Qwen3-1.4B	No Comp.	30.39	43.89	52.76	62.30	56.04	33.33	32.74	24.43	24.98	69.50	90.93	41.87	8.75	99.42	66.16	63.87	50.08	
	0.25	27.78	36.58	49.92	51.68	45.59	27.28	32.95	24.19	24.74	69.50	87.77	41.12	13.50	98.08	59.37	55.65	46.61	
	0.50	25.05	30.04	45.26	40.15	35.99	21.38	28.82	23.19	22.84	56.50	85.77	38.79	12.00	94.83	40.40	50.48	40.72	
	0.75	21.53	21.56	34.26	25.28	28.31	14.90	20.24	21.20	15.69	31.50	84.27	34.69	10.00	83.00	20.63	48.67	32.23	
	0.90	12.52	11.94	24.86	19.12	24.55	5.80	11.83	19.78	6.88	2.50	83.50	30.54	10.00	39.00	11.26	49.31	22.71	
	0.25	29.85	41.81	52.99	60.60	52.18	34.47	31.79	24.05	24.70	71.50	90.93	42.05	7.50	99.75	64.24	63.29	49.48	
	0.50	29.44	40.32	50.18	58.68	46.87	34.74	29.92	23.71	23.47	68.50	91.12	39.06	6.62	99.75	61.95	59.66	47.75	
	0.75	25.18	29.74	37.92	44.52	36.72	23.61	25.13	22.39	18.95	55.50	90.66	37.42	10.55	98.53	49.01	56.28	41.38	
	0.90	21.13	17.32	27.50	33.18	27.48	12.47	20.27	19.17	13.59	15.92	90.07	35.49	8.06	83.71	37.79	55.94	32.44	
	0.25	30.30	43.48	52.83	62.09	55.71	33.29	32.39	23.91	24.72	71.00	90.93	42.02	8.25	99.42	66.37	64.28	50.06	
	0.50	30.37	43.59	52.53	61.95	54.06	34.46	31.23	24.10	23.61	70.50	91.10	41.90	8.50	98.83	66.34	63.81	49.81	
	0.75	31.13	41.17	51.30	62.81	53.77	36.23	29.65	24.25	21.40	67.75	91.07	41.46	7.20	99.58	64.52	63.73	49.13	
	0.90	30.47	36.76	50.08	63.97	48.27	36.04	24.56	23.25	17.75	48.00	91.44	40.83	9.62	97.50	60.91	61.56	46.29	
	0.25	28.73	43.50	53.01	61.57	55.37	32.46	32.32	24.13	24.78	70.50	91.06	41.81	7.35	99.42	66.39	64.27	49.79	
	0.50	28.89	43.00	51.70	62.67	53.38	35.57	31.33	23.91	23.91	68.50	91.02	38.60	7.22	98.47	65.79	60.16	49.01	
	0.75	28.64	43.39	50.61	62.07	53.29	35.73	30.73	23.60	23.05	65.50	91.02	38.92	7.81	97.75	65.35	60.63	48.63	
	0.90	29.86	42.65	50.21	61.96	52.55	36.31	28.16	23.50	20.17	57.42	90.41	40.08	7.10	96.29	63.62	62.13	47.65	
	0.25	30.23	43.49	52.16	62.23	54.77	33.32	32.69	24.48	24.83	70.00	91.10	41.62	7.95	99.17	66.22	64.12	49.90	
	0.50	30.59	43.36	51.93	62.58	54.61	33.39	32.91	24.71	24.87	71.50	91.10	41.85	9.55	97.17	65.16	64.35	49.98	
	0.75	31.01	43.70	52.81	63.94	53.10	33.32	32.50	24.99	24.83	73.50	91.08	40.41	8.53	99.55	63.53	63.58	49.13	
	0.90	28.14	38.72	52.82	62.11	44.31	29.59	30.44	24.26	23.96	62.00	89.83	37.87	6.97	98.33	34.63	61.98	44.75	
	0.25	29.77	43.44	52.45	60.91	54.52	31.30	32.58	24.31	25.11	69.00	91.06	41.60	7.85	100.00	65.94	63.49	49.58	
	0.50	29.26	42.33	51.80	61.51	51.89	34.80	31.51	23.94	24.49	67.00	90.87	40.47	7.97	99.75	63.35	60.16	48.82	
	0.75	29.93	43.24	51.75	62.07	51.65	32.54	31.49	24.04	24.36	72.50	90.62	40.06	9.70	97.53	63.24	61.45	49.14	
	0.90	31.85	39.00	53.82	60.74	47.52	33.74	30.05	24.14	24.01	67.00	91.47	36.60	7.84	97.67	53.09	61.87	47.53	
	0.25	30.22	44.72	53.48	64.23	57.14	37.73	32.46	24.01	24.99	73.00	90.43	42.39	9.56	98.27	66.81	63.77	50.83	
	0.50	29.71	41.64	51.70	64.46	55.08	38.02	30.59	23.78	23.10	71.00	90.43	42.10	9.03	99.27	65.50	63.82	49.82	
	0.75	30.02	41.28	51.89	63.97	52.06	37.32	28.72	23.27	21.30	62.50	90.46	41.67	7.76	98.52	64.40	62.51	48.60	
	0.90	29.20	36.79	49.56	62.71	47.65	35.42	24.46	22.56	17.64	48.								

KVzip) score tokens using properties intrinsic to the context itself (i.e., key geometric diversity for KeyDiff and semantic redundancy for KVzip) without access to the query. For each baseline, the corresponding “+ VECTOR” variant retains the original importance scorer and augments it with the reconstructability-aware approximation tier.

Models We report results on three open-source models: Llama-3.1-8B-Instruct [1], Qwen3-14B [32], and Qwen3-0.6B [32].

Benchmarks We use LongBench [33] as the primary quantitative benchmark and Needle-in-a-Haystack (NIAH) [34] as a stress test for long-range retrieval. For LongBench, we evaluate on a 16-task subset obtained by excluding the 5 Chinese-language tasks from the original 21-task collection, using the full test split.

Metrics LongBench tasks are evaluated with their official task-specific metrics (F1, ROUGE-L, exact match / accuracy, and edit similarity); we report Avg as the arithmetic mean over the 16 selected tasks. We evaluate compression ratios $p_c \in \{0.25, 0.50, 0.75, 0.90\}$, with the corresponding approximation ratios set by Eq. (1): $p_a \in \{0.125, 0.25, 0.125, 0.05\}$, respectively.

More implementation and reproducibility details are provided in Appendix C.

5.2 LongBench Main Results

Table 2 reports full LongBench results. Overall, augmenting eviction baselines with VECTOR improves downstream performance in most high-compression settings, with gains most consistent at $p_c \in \{0.75, 0.90\}$. At lower compression ratios, the approximation tier provides limited additional benefit, as the base eviction policy already retains most contextually relevant tokens.

The strongest and most consistent improvements are observed with the two query-agnostic baselines, KeyDiff and KVzip. For KeyDiff, gains are particularly pronounced at high compression: on Qwen3-14B, KeyDiff+VECTOR improves the average score by +7.03 points at $p_c=0.50$, +9.15 at $p_c=0.75$, and +9.73 at $p_c=0.90$; Similar gains are observed on Qwen3-0.6B (Appendix A). KVzip+VECTOR delivers consistent improvements at high compression across all three models, reaching +3.97 points on Llama-3.1-8B at $p_c=0.90$. These results support the central claim of this work: introducing a reconstructability-aware approximation tier can recover a substantial portion of the information that would otherwise be irretrievably lost under binary eviction. This benefit is most pronounced for query-agnostic baselines under high compression, where importance and reconstructability capture largely orthogonal dimensions of utility.

For the two query-aware baselines, SnapKV and PyramidKV, improvements are more modest and mixed. SnapKV+VECTOR yields marginal or slightly negative effects at moderate compression ratios but consistent gains at $p_c=0.90$ across all three models; PyramidKV results are more variable, with no clear improvement trend across models or compression levels. We attribute this to the fact that query-aware methods already preserve the most pertinent context tokens, leaving limited headroom for the approximation tier. This is consistent with Proposition 1: when evicted tokens carry negligible importance ($w^* \ll \bar{w}$), the required R_{approx}^2 threshold rises, making net gains harder to achieve.

5.3 Sensitivity to Approximation Ratio

We study how downstream performance varies with the approximation ratio p_a under three compression ratios $p_c \in \{0.50, 0.75, 0.90\}$. We sweep p_a in increments of 0.05 using KeyDiff and KVzip on two LongBench tasks (HotpotQA and NarrativeQA) with Llama-3.1-8B-Instruct, and report the mean score averaged across all four combinations. Figure 3 shows the results.

Across all three compression ratios, performance generally rises as p_a increases from zero, then falls as p_a approaches its upper limit. The trend is clearest at higher compression ratios. Specifically, at $p_c = 0.50$, the formula value $p_a = 0.25$ falls within the high-performing region. Compared to $p_a = 0$ and $p_a = 0.5$, the downstream performance increases from 43.6% to 45.5%, and then decreases to

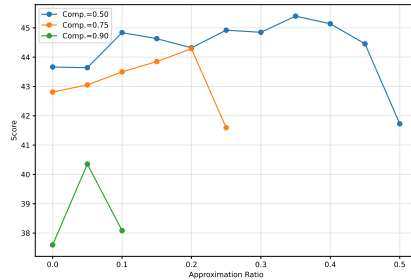


Figure 3: Mean LongBench score vs. approximation ratio p_a under three compression ratios, averaged over two baselines (KeyDiff, KVzip) and two tasks (HotpotQA, NarrativeQA) on Llama-3.1-8B-Instruct.

41.8%. At $p_c = 0.75$, performance rises steadily up to $p_a = 0.20$ (from 42.9% to 44.3%), then collapses sharply at $p_a = 0.25$ to only 41.6%. At $p_c = 0.90$, the peak is at $p_a = 0.05$ (40.5%).

These results support the intuition behind three-way allocation. When p_a is too small, few tokens enter the Approximation tier. Recoverable information that would otherwise be lost under binary eviction remains unrecovered. When p_a is too large, two problems arise. The Retention tier shrinks, forcing tokens that are hard to reconstruct into approximation. At the same time, easy-to-reconstruct tokens with low importance are approximated instead of evicted, wasting budget. A moderate p_a balances these two effects and leads to a better downstream performance.

5.4 Needle-in-a-Haystack Experiments

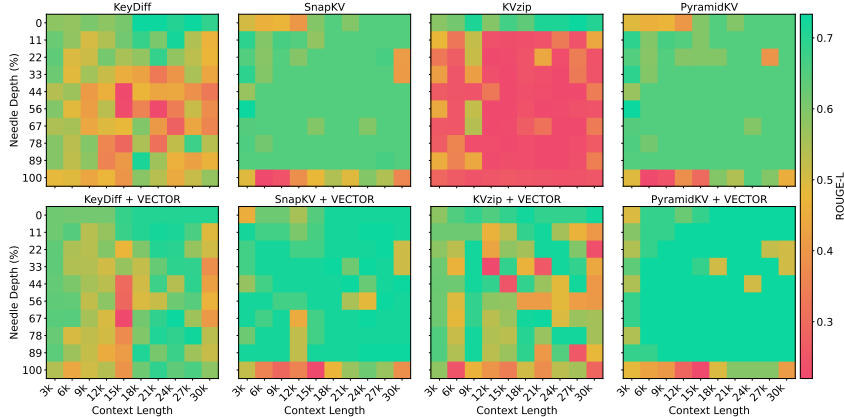


Figure 4: NIAH heatmaps on Llama-3.1-8B at $p_c=0.90$. *Top row*: KeyDiff, SnapKV, KVzip, and PyramidKV. *Bottom row*: corresponding VECTOR-augmented variants.

To further assess retrieval robustness under strict memory budgets, we evaluate NIAH on Llama-3.1-8B across all four baselines and their VECTOR-augmented variants. We focus on the high-compression regime $p_c=0.90$ (with $p_a=0.05$ per Eq. (1)), where differences between methods are most pronounced. We use a 10×10 grid over context lengths $\{3k, 6k, \dots, 30k\}$ and needle depths $\{0, 11, 22, \dots, 100\}\%$; each cell is averaged over 5 independent runs and reported as ROUGE-L F1. Figure 4 shows the resulting heatmaps.

Across all four baseline families, VECTOR consistently improves retrieval quality, though the magnitude of gain varies by baseline. The largest improvement is observed for KVzip, where the baseline exhibits broad low-score regions and KVzip+VECTOR substantially recovers performance across both context lengths and needle depths. For KeyDiff, VECTOR provides clear gains, primarily lifting low-score cells at harder depth-length combinations. For SnapKV and PyramidKV, whose baselines are already strong at this compression ratio, improvements are more moderate but consistently positive, in line with the reduced-headroom pattern observed on LongBench.

Overall, these results further support the role of reconstructability-aware approximation under tight memory budgets: rather than merely shifting average scores upward, VECTOR changes the failure pattern from large contiguous low-score regions to more localized difficult cells, indicating improved robustness under challenging retrieval conditions.

6 Conclusion

We propose VECTOR, a lightweight three-way allocation framework that integrates reconstructability-aware approximation into existing eviction methods. By separating token importance from reconstructability, VECTOR extends binary retain/evict decisions into retention, approximation, and eviction under the same memory budget. The design is practical: value approximation is implemented with offline OLS calibration and does not require model retraining. Theoretical discussions are provided to connect the OLS R^2 with the compression performance. Empirically, augmenting representative baselines with VECTOR improves long-context performance in most high-compression settings and yields more robust retrieval behavior in NIAH. These results suggest that combining

importance-aware eviction with reconstructability-aware approximation is a promising direction for future long-context inference systems.

Limitations VECTOR has some limitations. First, p_a is set by an empirical formula (Eq. (1)) rather than optimized per-sample or per-layer. This may leave room for improvement, particularly for tasks or models where the optimal p_a deviates from the formula. Second, gains over query-aware baselines such as SnapKV and PyramidKV are modest. These methods already preserve query-relevant tokens effectively, leaving limited headroom for the approximation tier. To improve, scorer-aware allocation and adaptive approximation ratios can be potential future directions.

References

- [1] Aaron Grattafiori, Abhimanyu Dubey, Abhinav Jauhri, Abhinav Pandey, Abhishek Kadian, Ahmad Al-Dahle, Aiesha Letman, Akhil Mathur, Alan Schelten, Alex Vaughan, et al. The llama 3 herd of models. *arXiv preprint arXiv:2407.21783*, 2024.
- [2] Gemini Team, Petko Georgiev, Ving Ian Lei, Ryan Burnell, Libin Bai, Anmol Gulati, Garrett Tanzer, Damien Vincent, Zhufeng Pan, Shibo Wang, et al. Gemini 1.5: Unlocking multimodal understanding across millions of tokens of context. *arXiv preprint arXiv:2403.05530*, 2024.
- [3] Aaditya Singh, Adam Fry, Adam Perelman, Adam Tart, Adi Ganesh, Ahmed El-Kishky, Aidan McLaughlin, Aiden Low, AJ Ostrow, Akhila Ananthram, et al. Openai gpt-5 system card. *arXiv preprint arXiv:2601.03267*, 2025.
- [4] Woosuk Kwon, Zhuohan Li, Siyuan Zhuang, Ying Sheng, Lianmin Zheng, Cody Hao Yu, Joseph Gonzalez, Hao Zhang, and Ion Stoica. Efficient memory management for large language model serving with pagedattention. In *Proceedings of the 29th symposium on operating systems principles*, pages 611–626, 2023.
- [5] Zhenyu Zhang, Ying Sheng, Tianyi Zhou, Tianlong Chen, Lianmin Zheng, Ruisi Cai, Zhao Song, Yuandong Tian, Christopher Ré, Clark Barrett, et al. H2o: Heavy-hitter oracle for efficient generative inference of large language models. *Advances in Neural Information Processing Systems*, 36:34661–34710, 2023.
- [6] Patrick Lewis, Ethan Perez, Aleksandra Piktus, Fabio Petroni, Vladimir Karpukhin, Naman Goyal, Heinrich Küttler, Mike Lewis, Wen-tau Yih, Tim Rocktäschel, et al. Retrieval-augmented generation for knowledge-intensive nlp tasks. *Advances in neural information processing systems*, 33:9459–9474, 2020.
- [7] Shunyu Yao, Jeffrey Zhao, Dian Yu, Nan Du, Izhak Shafran, Karthik Narasimhan, and Yuan Cao. React: Synergizing reasoning and acting in language models. *arXiv preprint arXiv:2210.03629*, 2022.
- [8] Charles Packer, Vivian Fang, Shishir_G Patil, Kevin Lin, Sarah Wooders, and Joseph_E Gonzalez. Memgpt: towards llms as operating systems. 2023.
- [9] Yuhong Li, Yingbing Huang, Bowen Yang, Bharat Venkitesh, Acyr Locatelli, Hanchen Ye, Tianle Cai, Patrick Lewis, and Deming Chen. Snapkv: Llm knows what you are looking for before generation. *Advances in Neural Information Processing Systems*, 37:22947–22970, 2024.
- [10] Junyoung Park, Dalton Jones, Matthew J Morse, Raghavv Goel, Mingu Lee, and Chris Lott. Keydiff: Key similarity-based kv cache eviction for long-context llm inference in resource-constrained environments. *arXiv preprint arXiv:2504.15364*, 2025.
- [11] Jang-Hyun Kim, Jinuk Kim, Sangwoo Kwon, Jae W Lee, Sangdoo Yun, and Hyun Oh Song. Kvzip: Query-agnostic kv cache compression with context reconstruction. *arXiv preprint arXiv:2505.23416*, 2025.
- [12] Jianlong Lei and Shashikant Ilager. Arkv: Adaptive and resource-efficient kv cache management under limited memory budget for long-context inference in llms. *arXiv preprint arXiv:2603.08727*, 2026.

- [13] Zhongwei Wan, Xinjian Wu, Yu Zhang, Yi Xin, Chaofan Tao, Zhihong Zhu, Xin Wang, Siqi Luo, Jing Xiong, and Mi Zhang. D2o: Dynamic discriminative operations for efficient generative inference of large language models. *arXiv preprint arXiv:2406.13035*, 2, 2024.
- [14] Alina Shutova, Vladimir Malinovskii, Vage Egiazarian, Denis Kuznedelev, Denis Mazur, Nikita Surkov, Ivan Ermakov, and Dan Alistarh. Cache me if you must: Adaptive key-value quantization for large language models. *arXiv preprint arXiv:2501.19392*, 2025.
- [15] Yuhao Zhou, Sirui Song, Boyang Liu, Zhiheng Xi, Senjie Jin, Xiaoran Fan, Zhihao Zhang, Wei Li, and Xuanjing Huang. Elitekv: Scalable kv cache compression via rope frequency selection and joint low-rank projection. *arXiv preprint arXiv:2503.01586*, 2025.
- [16] Jitai Hao, Qiang Huang, Yaowei Wang, Min Zhang, and Jun Yu. Deltakv: Residual-based kv cache compression via long-range similarity. *arXiv preprint arXiv:2602.08005*, 2026.
- [17] Adam Zweiger, Xinghong Fu, Han Guo, and Yoon Kim. Fast kv compaction via attention matching. *arXiv preprint arXiv:2602.16284*, 2026.
- [18] Zirui Liu, Jiayi Yuan, Hongye Jin, Shaochen Zhong, Zhaozhuo Xu, Vladimir Braverman, Beidi Chen, and Xia Hu. Kivi: A tuning-free asymmetric 2bit quantization for kv cache. *arXiv preprint arXiv:2402.02750*, 2024.
- [19] Xing Li, Zeyu Xing, Yiming Li, Linping Qu, Hui-Ling Zhen, Wulong Liu, Yiwu Yao, Sinno Jialin Pan, and Mingxuan Yuan. Kvtuner: Sensitivity-aware layer-wise mixed-precision kv cache quantization for efficient and nearly lossless llm inference. *arXiv preprint arXiv:2502.04420*, 2025.
- [20] Zefan Cai, Yichi Zhang, Bofei Gao, Yuliang Liu, Yucheng Li, Tianyu Liu, Keming Lu, Wayne Xiong, Yue Dong, Junjie Hu, et al. Pyramidkv: Dynamic kv cache compression based on pyramidal information funneling. *arXiv preprint arXiv:2406.02069*, 2024.
- [21] Hao Kang, Qingru Zhang, Souvik Kundu, Geonhwa Jeong, Zaoxing Liu, Tushar Krishna, and Tuo Zhao. Gear: An efficient kv cache compression recipe for near-lossless generative inference of llm. *arXiv preprint arXiv:2403.05527*, 2024.
- [22] Chi-Chih Chang, Wei-Cheng Lin, Chien-Yu Lin, Chong-Yan Chen, Yu-Fang Hu, Pei-Shuo Wang, Ning-Chi Huang, Luis Ceze, Mohamed S Abdelfattah, and Kai-Chiang Wu. Palu: Kv-cache compression with low-rank projection. In *The Thirteenth International Conference on Learning Representations*, 2025.
- [23] Aixin Liu, Bei Feng, Bin Wang, Bingxuan Wang, Bo Liu, Chenggang Zhao, Chengqi Deng, Chong Ruan, Damai Dai, Daya Guo, et al. Deepseek-v2: A strong, economical, and efficient mixture-of-experts language model. *arXiv preprint arXiv:2405.04434*, 2024.
- [24] Dipkumar Patel. Turboangle: Near-lossless kv cache compression via uniform angle quantization. *arXiv preprint arXiv:2603.27467*, 2026.
- [25] Jesse Dodge, Maarten Sap, Ana Marasović, William Agnew, Gabriel Ilharco, Dirk Groeneveld, Margaret Mitchell, and Matt Gardner. Documenting large webtext corpora: A case study on the colossal clean crawled corpus. In *Proceedings of the 2021 conference on empirical methods in natural language processing*, pages 1286–1305, 2021.
- [26] Ashish Vaswani, Noam Shazeer, Niki Parmar, Jakob Uszkoreit, Llion Jones, Aidan N Gomez, Łukasz Kaiser, and Illia Polosukhin. Attention is all you need. *Advances in neural information processing systems*, 30, 2017.
- [27] Noam Shazeer. Fast transformer decoding: One write-head is all you need. *arXiv preprint arXiv:1911.02150*, 2019.
- [28] Joshua Ainslie, James Lee-Thorp, Michiel De Jong, Yury Zemlyanskiy, Federico Lebrón, and Sumit Sanghai. Gqa: Training generalized multi-query transformer models from multi-head checkpoints. In *Proceedings of the 2023 Conference on Empirical Methods in Natural Language Processing*, pages 4895–4901, 2023.

- [29] Mingjie Sun, Xinlei Chen, J Zico Kolter, and Zhuang Liu. Massive activations in large language models. *arXiv preprint arXiv:2402.17762*, 2024.
- [30] Jianlin Su, Murtadha Ahmed, Yu Lu, Shengfeng Pan, Wen Bo, and Yunfeng Liu. Roformer: Enhanced transformer with rotary position embedding. *Neurocomputing*, 568:127063, 2024.
- [31] Alessio Devoto, Maximilian Jeblick, and Simon Jégou. Expected attention: Kv cache compression by estimating attention from future queries distribution. *arXiv preprint arXiv:2510.00636*, 2025.
- [32] An Yang, Anfeng Li, Baosong Yang, Beichen Zhang, Binyuan Hui, Bo Zheng, Bowen Yu, Chang Gao, Chengen Huang, Chenxu Lv, et al. Qwen3 technical report. *arXiv preprint arXiv:2505.09388*, 2025.
- [33] Yushi Bai, Xin Lv, Jiajie Zhang, Hongchang Lyu, Jiankai Tang, Zhidian Huang, Zhengxiao Du, Xiao Liu, Aohan Zeng, Lei Hou, et al. Longbench: A bilingual, multitask benchmark for long context understanding. In *Proceedings of the 62nd annual meeting of the association for computational linguistics (volume 1: Long papers)*, pages 3119–3137, 2024.
- [34] Greg Kamradt. Llmtest_needleinahaystack. https://github.com/gkamradt/LLMTest_NeedleInAHaystack, 2023. GitHub repository, accessed 2026-04-20.
- [35] NVIDIA. kvpress. <https://github.com/NVIDIA/kvpress>, 2025. GitHub repository, accessed 2026-04-20.

A Additional Results

Table 3: LongBench results for four eviction baselines and their VECTOR-augmented variants on Qwen3-0.6B, under compression ratios $p_c \in \{0.25, 0.50, 0.75, 0.90\}$. Approximation ratios are set by Eq. 1. Experimental setup follows Table 2.

Method	Comp. Ratio	LongBench																	Avg.
		narrativeqa	qasper	multifield-qa_en	hotpotqa	2wikimqa	musique	gov_report	qmsum	multi_news	tree	triviaqa	samsun	passage_count	passage_retrieval_en	lcc	repobench-p		
Qwen3-0.6B	No Comp.	15.71	18.59	46.77	35.60	29.52	14.47	27.06	20.52	24.36	20.00	70.42	35.13	0.50	75.00	31.79	29.42	30.93	
	0.25	15.20	15.83	36.94	25.09	26.05	7.78	25.86	19.74	23.02	54.50	66.70	33.17	0.62	37.50	29.63	31.36	28.06	
	0.50	12.09	11.47	29.91	16.70	24.98	5.66	20.06	19.24	17.83	46.00	62.76	32.18	0.28	15.00	25.83	30.16	23.13	
	0.75	10.30	7.71	25.17	12.66	19.48	4.29	11.89	18.19	10.30	12.50	59.62	28.04	0.50	6.00	13.41	27.41	16.72	
	0.90	6.27	4.83	21.81	9.80	20.29	3.69	6.36	18.12	5.97	1.50	52.63	22.28	0.85	5.00	7.64	26.70	13.36	
KeyDiff	0.25	17.07	18.56	45.54	32.10	31.04	11.36	25.73	20.54	23.14	27.00	68.89	33.75	1.00	68.00	30.52	29.69	30.25	
	0.50	18.00	16.59	38.60	29.27	27.86	11.42	23.28	20.44	21.59	38.50	69.47	34.18	1.50	54.00	27.67	30.21	28.91	
	0.75	14.85	12.53	26.85	20.08	21.58	7.00	16.91	19.61	15.21	33.50	67.99	34.05	1.00	19.00	25.01	30.86	22.88	
	0.90	8.80	13.43	23.16	16.86	26.93	5.22	12.82	18.96	10.75	14.00	64.78	32.94	1.53	5.00	16.55	31.33	18.94	
KeyDiff + VECTOR	0.25	15.41	18.50	46.66	37.12	30.04	14.66	26.88	20.56	23.39	20.00	70.61	33.82	1.00	74.50	30.58	29.06	30.80	
	0.50	15.69	18.31	46.54	36.82	30.01	13.99	25.06	20.63	21.99	30.00	70.32	33.49	0.50	75.00	31.12	29.37	31.18	
	0.75	15.98	17.09	45.31	37.13	30.28	12.81	22.15	20.17	19.05	30.50	70.68	32.56	0.50	77.00	34.00	31.66	31.05	
	0.90	16.82	15.85	39.96	37.25	29.73	12.74	17.53	19.39	14.46	23.50	71.89	32.24	1.00	75.50	35.61	34.17	29.85	
SnapKV	0.25	15.76	18.80	46.88	36.99	29.56	14.54	26.98	20.55	23.85	21.50	70.76	34.53	0.50	74.00	31.05	29.57	30.99	
	0.50	15.78	17.98	46.92	35.64	28.64	15.20	26.69	20.68	23.65	19.00	70.40	34.75	0.50	75.00	28.32	28.42	30.47	
	0.75	16.79	17.14	45.31	35.38	30.64	13.90	25.39	20.58	22.12	29.50	69.87	35.65	0.50	76.00	27.99	28.62	30.96	
	0.90	17.57	16.33	45.26	36.83	27.15	13.98	23.39	20.09	19.34	37.00	69.70	34.63	0.50	78.00	32.79	31.15	31.48	
SnapKV + VECTOR	0.25	15.95	18.26	46.78	36.45	29.65	14.61	27.21	20.32	24.14	20.00	70.10	34.67	1.00	74.00	30.88	29.22	30.83	
	0.50	15.63	16.92	48.64	35.34	30.56	14.86	27.27	20.23	24.28	27.00	70.68	34.53	0.50	75.00	30.64	30.12	31.39	
	0.75	13.77	14.41	45.42	33.25	31.32	10.66	26.18	20.37	24.46	54.50	69.72	33.93	0.50	28.50	31.48	30.39	29.30	
	0.90	12.74	15.93	37.63	18.74	28.31	5.90	23.55	19.79	22.06	45.50	67.34	30.21	0.00	11.00	20.82	28.95	24.28	
KVzip	0.25	16.03	18.99	46.46	35.73	28.43	14.15	27.33	20.67	23.92	23.00	70.17	35.36	0.50	75.00	30.23	29.29	30.95	
	0.50	15.68	17.71	45.41	33.80	29.33	12.52	26.50	20.86	23.77	21.50	70.03	35.96	0.50	70.00	27.05	28.82	29.96	
	0.75	15.66	16.15	47.52	34.60	30.30	13.68	26.56	20.73	24.19	44.00	69.64	35.11	0.50	69.00	26.82	29.32	31.45	
	0.90	14.08	15.68	42.87	26.00	30.16	6.46	25.40	20.42	23.35	55.00	69.76	33.23	0.00	15.50	25.10	29.76	27.05	
KVzip + VECTOR	0.25	15.69	15.24	46.01	29.62	24.43	11.38	25.90	21.33	22.96	4.50	62.82	16.65	3.00	67.00	27.47	25.87	26.24	
	0.50	16.12	13.47	44.18	30.51	23.60	8.34	22.04	20.82	18.66	4.00	62.86	20.80	3.00	65.00	26.74	27.22	25.46	
	0.75	16.70	15.09	42.33	30.35	24.68	9.49	19.84	19.87	18.81	17.50	66.89	24.97	3.00	63.50	33.45	27.77	27.14	
	0.90	16.75	16.55	38.99	30.78	30.00	7.29	16.98	19.34	14.46	23.50	70.72	30.03	1.00	68.50	35.55	32.26	28.29	
PyramidKV	0.25	16.60	15.89	45.92	28.82	24.79	10.63	26.12	20.65	23.24	4.50	63.25	18.51	3.00	67.00	26.20	25.88	26.31	
	0.50	17.17	13.72	44.70	29.50	24.08	9.85	24.32	21.07	20.82	10.50	63.93	19.45	2.50	67.50	25.39	25.82	26.27	
	0.75	16.61	13.30	42.67	29.29	23.38	7.99	22.27	20.32	17.76	12.50	61.41	18.82	3.00	65.50	23.90	25.88	25.29	
	0.90	16.15	14.89	37.49	27.55	19.77	7.92	19.17	19.80	13.94	13.50	60.80	21.43	3.00	63.50	23.73	26.10	24.30	
PyramidKV + VECTOR																			

B Proofs

B.1 Proof of Proposition 1

Given the formula for \mathcal{E} and μ_A , we have

$$\mathcal{E}(p_a, p_c) \approx \sum_{i \in \mathcal{I}_E(p_a, p_c)} w_i + \left(\sum_{i \in \mathcal{I}_A(p_a, p_c)} w_i \right) (1 - R_{\text{approx}}^2(p_a, p_c)). \quad (2)$$

Since w^* is the importance score at the truncation boundary, \mathcal{I}_E has proportion $p_c - p_a$, and \mathcal{I}_A contains $2p_a$ proportion of tokens, we have

$$\sum_{i \in \mathcal{I}_E(p_a + \delta, p_c)} w_i - \sum_{i \in \mathcal{I}_E(p_a, p_c)} w_i \approx -w^* \delta, \quad (3)$$

i.e., increasing p_a by δ removes δ boundary tokens with weight w^* from \mathcal{I}_E . Similarly,

$$\sum_{i \in \mathcal{I}_A(p_a + \delta, p_c)} w_i - \sum_{i \in \mathcal{I}_A(p_a, p_c)} w_i \approx (w^* + \bar{w}) \delta, \quad (4)$$

since $|\mathcal{I}_A|$ grows by 2δ : δ tokens enter from \mathcal{I}_E with weight w^* , and δ tokens enter from the *Retention* set with weight $\approx \bar{w}$. The latter holds because the partition between *Approximation* and *Retention* is determined by reconstruction error rather than importance score, so the transferred tokens carry average weight \bar{w} .

Combining the above, we obtain:

$$\mathcal{E}(p_a + \delta, p_c) - \mathcal{E}(p_a, p_c) \approx -w^* \delta + (w^* + \bar{w}) \delta (1 - R_{\text{approx}}^2(p_a, p_c)) - 2p_a \bar{w} \delta \frac{\partial R_{\text{approx}}^2}{\partial p_a}. \quad (5)$$

For $\mathcal{E}(p_a + \delta, p_c) < \mathcal{E}(p_a, p_c)$ (with $\delta > 0$), we require:

$$-w^* + (w^* + \bar{w})(1 - R_{\text{approx}}^2) - 2p_a\bar{w}\frac{\partial R_{\text{approx}}^2}{\partial p_a} < 0 \quad (6)$$

$$\Leftrightarrow (w^* + \bar{w})(1 - R_{\text{approx}}^2) < w^* + 2p_a\bar{w}\frac{\partial R_{\text{approx}}^2}{\partial p_a} \quad (7)$$

$$\Leftrightarrow 1 - R_{\text{approx}}^2 < \frac{w^* + 2p_a\bar{w}\frac{\partial R_{\text{approx}}^2}{\partial p_a}}{w^* + \bar{w}} \quad (8)$$

$$\Leftrightarrow R_{\text{approx}}^2 > 1 - \frac{w^* + 2p_a\bar{w}\frac{\partial R_{\text{approx}}^2}{\partial p_a}}{w^* + \bar{w}}. \quad (9)$$

For small p_a , the term $2p_a\bar{w}\frac{\partial R_{\text{approx}}^2}{\partial p_a}$ is negligible, yielding:

$$R_{\text{approx}}^2(p_a, p_c) > 1 - \frac{w^*}{w^* + \bar{w}} = \frac{\bar{w}}{w^* + \bar{w}}. \quad \square$$

B.2 Proof of Example 1

Since the selection of $\mathcal{I}_E(p_a, p_c)$ is independent of the reconstruction error, the signed residuals r_i of non-evicted tokens follow the same $\mathcal{N}(0, \sigma^2)$ distribution. Further invoking the independence between r_i^2 and w_i , the overall distortion is:

$$\mathcal{E}(p_a, p_c) = \sum_{i \in \mathcal{I}_E(p_a, p_c)} w_i + \frac{1}{\Sigma^2} \sum_{i \in \mathcal{I}_A(p_a, p_c)} w_i r_i^2 \quad (10)$$

$$\approx \sum_{i \in \mathcal{I}_E(p_a, p_c)} w_i + \frac{2p_a\bar{w}}{\Sigma^2} \cdot \frac{\sum_{i \in \mathcal{I}_A(p_a, p_c)} r_i^2}{|\mathcal{I}_A(p_a, p_c)|}. \quad (11)$$

Since the *Approximation* set selects the $2p_a$ tokens with the smallest reconstruction errors (i.e., those with $|r_i| \leq \eta(p_a, p_c)$), corresponding to the central $2p_a/(1 - p_c + p_a)$ fraction of the Gaussian distribution, the conditional distribution of r_i given $i \in \mathcal{I}_A(p_a, p_c)$ is a truncated normal on $[-\eta(p_a, p_c), \eta(p_a, p_c)]$, where $\eta(p_a, p_c) = \sigma\Phi^{-1}(1/2 + p_a/(1 - p_c + p_a))$, and $2\Phi(\eta/\sigma) - 1 = 2p_a/(1 - p_c + p_a)$.

Recalling that for $X \sim \mathcal{N}(0, \sigma^2)$:

$$\mathbb{E}(X^2 \mid |X| \leq x) = \sigma^2 \left[1 - \frac{2(x/\sigma)\phi(x/\sigma)}{2\Phi(x/\sigma) - 1} \right],$$

we obtain:

$$\mathcal{E}(p_a, p_c) \approx \sum_{i \in \mathcal{I}_E(p_a, p_c)} w_i + 2p_a\bar{w} \underbrace{\frac{\sigma^2}{\Sigma^2} \left(1 - \frac{2(\eta(p_a, p_c)/\sigma)\phi(\eta(p_a, p_c)/\sigma)}{2p_a/(1 - p_c + p_a)} \right)}_{1 - R_{\text{approx}}^2(p_a, p_c)}. \quad \square$$

C Reproducibility Details

We provide implementation details for reproducibility and checklist reporting.

C.1 LongBench Setup Details

- **Code base and framework.** All LongBench and NIAH experiments in this section use the KVPress evaluation framework and official baseline implementations [35].
- **Repository version.** KVPress commit hash: 91773cb8b5713fe6ad54e3e7a97dd343fb40d37b.
- **Model identifiers.** The evaluated models are meta-llama/Llama-3.1-8B-Instruct, Qwen/Qwen3-14B, and Qwen/Qwen3-0.6B.

- **Calibration protocol.** For each model, we perform one-time offline OLS calibration on C4 dataset [25]: 10,000 training sequences (length 4,096) are used to fit layer-wise $K \rightarrow V$ linear maps, and a held-out set of 100 sequences (length 4,096) is used for validation (Section 3.1). The calibrated W_{OLS} weights are fixed for all downstream experiments.
- **Benchmark split and coverage.** For LongBench, we evaluate the full test split of the 16-task English/code subset (i.e., 21 original tasks minus 5 Chinese tasks), and report the arithmetic mean over these 16 tasks.
- **Compression settings.** We evaluate $p_c \in \{0.25, 0.50, 0.75, 0.90\}$ and set p_a with Eq. 1, giving $p_a = \{0.125, 0.25, 0.125, 0.05\}$, respectively.
- **Randomness control.** We use a fixed random seed of 42 for all runs.
- **Inference protocol.** We use KVPress default inference behavior without additional decoding hyperparameter tuning; task-level generation limits follow the benchmark defaults in the KVPress pipeline.
- **Hardware.** Each experiment group can be run on a single NVIDIA H200 GPU.
- **Statistical reporting.** Due to the high computational cost of full-benchmark evaluation, all results are from one full run with fixed seed (no multi-seed repetition and no significance testing).

C.2 NIAH Setup Details

- **Model and methods.** NIAH is evaluated on meta-llama/Llama-3.1-8B-Instruct with KeyDiff, SnapKV, KVzip, PyramidKV, and their corresponding VECTOR-augmented variants.
- **Compression setting.** We report the high-compression setting $p_c = 0.90$ with $p_a = 0.05$ (Eq. 1).
- **Grid protocol.** We evaluate a 10×10 grid of context lengths $\{3000, 6000, \dots, 30000\}$ and needle depths $\{0, 11, 22, 33, 44, 56, 67, 78, 89, 100\}$.
- **Haystack construction.** Each grid cell uses 5 independent haystacks (`n_haystacks=5`) from `data/NIAH/PaulGrahamEssays`, with the default KVPress NIAH needle/question template.
- **Metric aggregation.** NIAH scores are ROUGE-L F1, averaged over the 5 haystacks per grid cell.
- **Method-specific query awareness.** We follow each method’s original setting: `query_aware` is enabled for SnapKV/PyramidKV (and their VECTOR variants) and disabled for KeyDiff/KVzip (and their VECTOR variants).
- **Inference and seed.** We use KVPress default inference behavior with fixed seed 42.

D Ablation Study: OLS vs. Analytical Pseudo-Inverse

We compare the $K \rightarrow V$ predictability of the data-driven OLS estimator against the MP pseudo-inverse. For each model, we report the mean and median R^2 aggregated across all layers, along with the fraction of layers where MP achieves $R^2 > 0$. OLS results match those in Table 1.

Table 4: OLS vs. MP pseudo-inverse: layer-aggregated R^2 on the held-out validation set. A negative R^2 indicates that the predictor performs worse than predicting the mean.

Model	OLS R^2		MP R^2		
	Mean	Median	Mean	Median	Layers with $R^2 > 0$
Llama-3.1-8B	0.697	0.690	0.511	0.508	100%
Qwen3-14B	0.695	0.691	-797.0	-1.545	30%
Qwen3-0.6B	0.939	0.936	-9250738	-2824	0%
Gemma-3-4B	0.890	0.897	-3.170	-0.767	29%
Qwen3-30B-A3B	0.686	0.720	-6987	-572.5	0%

OLS achieves positive R^2 on every layer of every model. MP, by contrast, fails systematically. On four of five models, MP produces negative R^2 on the majority of layers. On Qwen3-0.6B and Qwen3-30B-A3B, no layer achieves $R^2 > 0$ under MP. Aligning with the theoretical discussion in Section 3, these results confirm that MP does not minimize the V -prediction error.

E Ablation Study: V-only vs. K-only Approximation

VECTOR adopts a V-only approximation strategy, preserving exact keys and reconstructing values via OLS. A natural alternative is to flip this design: store values exactly and reconstruct keys instead. We refer to this variant as K-only approximation, which trains a $V \rightarrow K$ OLS estimator and applies forward RoPE to produce approximate keys.

We compare V-only (KeyDiff+VECTOR) and K-only against the KeyDiff baseline on four LongBench tasks using Llama-3.1-8B-Instruct. Both variants use identical budget, importance scorer, and three-way allocation logic, with p_a set by Eq. 1 as in the main experiments. The only difference is the approximation direction.

Table 5: V-only vs. K-only approximation on LongBench (Llama-3.1-8B-Instruct). KeyDiff is the unaugmented baseline. KeyDiff+VECTOR approximates values; KeyDiff+K-only approximates keys under the same memory budget.

Method	Comp. Ratio	Qasper	HotpotQA	2WikiMQA	Musique
KeyDiff	0.25	47.30	58.39	50.69	34.08
KeyDiff+VECTOR	0.25	48.18	58.45	50.72	33.59
KeyDiff+K-only	0.25	47.56	58.25	49.59	34.59
KeyDiff	0.50	45.65	56.07	46.20	28.62
KeyDiff+VECTOR	0.50	47.38	58.92	51.65	35.47
KeyDiff+K-only	0.50	43.70	54.31	49.18	30.55
KeyDiff	0.75	31.75	52.83	38.74	24.69
KeyDiff+VECTOR	0.75	39.20	54.83	45.85	28.83
KeyDiff+K-only	0.75	36.59	51.74	43.52	26.24
KeyDiff	0.90	17.00	40.03	26.18	16.01
KeyDiff+VECTOR	0.90	23.96	49.88	30.72	20.72
KeyDiff+K-only	0.90	21.44	38.93	26.37	17.77

Based on Table 5, at $p_c = 0.25$, the two variants perform similarly. As compression increases, their behaviors diverge. V-only approximation consistently improves over the KeyDiff baseline across all tasks and compression ratios. K-only approximation shows inconsistent gains. On HotpotQA, it falls below the baseline at $p_c = 0.50, 0.75$, and 0.90 . At $p_c = 0.90$, KeyDiff+VECTOR outperforms KeyDiff+K-only by 2.52 points on Qasper and 10.95 points on HotpotQA.

The performance gap is consistent with the asymmetric role of keys and values in attention. Reconstructed keys directly affect the softmax attention weights. Even small errors in keys are amplified nonlinearly by the softmax. This effect compounds under a higher compression ratio. Values, by contrast, enter only the linear weighted sum after softmax. They are substantially more tolerant to approximation error.